Biochemical and Biophysical Research Communications 435 (2013) 46–51

Contents lists available at SciVerse ScienceDirect

Biochemical and Biophysical Research Communications

journal homepage: www.elsevier.com/locate/ybbrc

Hypoxia-inducible factor 1α mediates the down-regulation of superoxide dismutase 2 in von Hippel–Lindau deficient renal clear cell carcinoma

Yao-Hui Gao [a,1], Cai-Xia Li [a,1], Shao-Ming Shen [a], Hui Li [a], Guo-Qiang Chen [a], Qing Wei [b,*], Li-Shun Wang [a,*]

[a] Shanghai Universities E-Institute for Chemical Biology, Key Laboratory of Cell Differentiation and Apoptosis of National Ministry of Education, Shanghai Jiaotong University School of Medicine (SJTU-SM), Shanghai 200025, PR China
[b] Department of Pathology, Ruijin Hospital, SJTU-SM, PR China

ARTICLE INFO

Article history:
Received 26 March 2013
Available online 20 April 2013

Keywords:
pVHL
HIF-1α
ROS
SOD2

ABSTRACT

Hypoxia-inducible factor 1α (HIF-1α) is an oxygen-sensitive subunit of HIF-1, the master transcription factor for cellular response to hypoxia. Down-regulation of the mitochondrial enzyme superoxide dismutase 2 (SOD2) contributes to the stabilization of HIF-1α under hypoxia due to the decreased dismutation of superoxide radical. Here we report that HIF-1α could also regulate the expression of SOD2. We found that both stabilization of HIF-1α expression under nomoxia caused by pVHL deficiency and hypoxia treatment significantly reduced SOD2 expression, and shRNAs specifically against HIF-1α restored SOD2 expression in both circumstances. Further analyses with luciferase reporter assay and chromatin immunoprecipitation assay revealed that HIF-1α inhibited and directly bound to the hypoxia-responsive element in SOD2 promoter. These findings indicated the existence of a positive feedback between HIF-1α and SOD2 and provided new clues for understanding the molecular mechanisms of hypoxia adaptation.

1. Introduction

Tumors generally possess hypoxic context because of the decreased blood supply caused by rapid proliferation of cancer cells. It has been well known the adaptation of cancer cells to hypoxia is mainly mediated by hypoxia-inducible factor 1 (HIF-1). HIF-1 is a heterodimeric transcription factor consisting of an oxygen-sensitive subunit HIF-1α and a constitutively expressed subunit HIF-1β.In normoxia, HIF-1α is hydroxylated by the PHDs. Hydroxylated HIF-1α is ubiquitinated and targeted for proteasomal degradation by the E3 ligase von Hippel-Lindau protein (pVHL) [1]. In hypoxia, cytosolic HIF-1α is stabilized due to the inhibition of hydroxylation and subsequently translocates into the nucleus, where it binds HIF-1β [2]. The HIF-1α/HIF-1β heterodimer binds to hypoxia-responsive elements (HREs) in the promoters of its target genes, such as vascular endothelial growth factor (VEGF) and pyruvate dehydrogenase 1(PDK1) [3–5]. These genes are involved in energy metabolism, angiogenesis, cell proliferation/differentiation and invasion/metastasis [6–8]. Hence, HIF-1α is recognized as an attractive target for the novel cancer therapeutics [6].

It is well known that hypoxic conditions can increase the level of intracellular reactive oxygen species (ROS) [9]. In turn, ROS can participate in signal transduction pathways that mediate HIF-1α stabilization [10,11]. Superoxide dismutase 2 (SOD2) is a primary antioxidant enzyme that catalyses the dismutation of superoxide radical. Recent studies have elucidated that ROS generated by SOD2 silencing increased HIF-1α expression [12]. But it is unknown whether HIF-1α regulates SOD2 conversely. Intriguingly, in a comparative proteomic analysis, we found that the expression of SOD2 decreased significantly in the pVHL deficient real clear carcinoma cell line RCC4. Further biochemical analyses indicated that HIF-1α regulated the expression of SOD2 through direct binding to its promoter. These findings raise the hypothesis that during hypoxia adaptation the regulation between HIF-1α and SOD2 is mutual.

2. Materials and methods

2.1. Cell culture and treatment

293T,RCC4 and RCC4/VHL were cultured in DMEM medium (Sigma–Aldrich, St Louis, MI, USA) supplemented with 10% FBS (Gibco BRL, Gaithersburg, MD, USA).SW620 and Caki-1 were respectively cultured in RPMI-1640 medium (Sigma–Aldrich, St Louis, MI, USA) and McCoy'5A(Invitrogen) with 10% FBS .RCC4 and RCC4/VHL were provided by Dr. J.K. Cheng in SJTU-SM. All cell lines were cultured in 5% CO_2/95% air in a humidified atmosphere at 37 °C. Hypoxic treatment was performed in a specially designed hypoxia incubator (Thermo Electron, Forma, MA, USA) with 1% O_2, 5% CO_2 and 93% N_2.

* Corresponding authors. Fax: +86 21 64154900 (L.-S. Wang).
E-mail addresses: weiqing1971@yahoo.com.cn (Q. Wei), jywangls@shsmu.edu.cn (L.-S. Wang).
[1] These two authors contribute equally to this work.

0006-291X/$ - see front matter Crown Copyright © 2013 Published by Elsevier Inc. All rights reserved.
http://dx.doi.org/10.1016/j.bbrc.2013.04.034

2.2. Isolation of mitochondria and protein extraction

Isolation of mitochondria was performed as described [13]. Briefly, 5×10^7 cells were used for isolation of mitochondria and the enriched mitochondria were dissolved in lysis buffer followed by centrifugation (35,000*g*, 1 h) at 4 °C. The supernatant was quantified using Bio-Rad RC-DC protein assay kit (Bio-Rad, Hercules, CA) and aliquoted. The protein samples were stored at −80 °C until analysis.

2.3. Protein labeling and two-dimensional gel electrophoresis

Shortly, 50 μg of mitochondrial protein of RCC4 and RCC4/VHL was minimally labeled with 400 pmol of either Cy3 or Cy5 for comparison on the same two-dimensional (2-D) gel. Internal standard was a mixture of 25 μg protein from each sample and was labeled with Cy2. The Cy2, Cy3 and Cy5-labeled samples were then applied to the same 17 cm IPG strip for IEF. Once the IEF was completed, the IPG strip was equilibrated followed by reduction. The second-dimensional separation was carried out on a 12% SDS–polyacrylamide gel. The Gel was run at 16 mA/gel for 30 min, and then 24 mA/gel until the dye reached the bottom of the gel. Three batches of samples were collected and analyzed following the same procedure.

2.4. Image analysis and in-gel digestion

Spot detection was performed using the DeCyder software (Version 6.5). Differential in-gel analysis (DIA) module was done by setting the target spot number to 1000. Differentially expressed spots with an absolute ratio of at least 1.5-fold were selected. The statistical analysis was calculated by the DeCyder software (version 6.5). The preparative gel was stained with Coomassie blue. Proteins of interest were excised, transferred into the ZipPlate micro-SPE Platewells (Millipore, Billerica, MA) and digested as described previously [7].

2.5. Mass spectrometry and protein identification

Protein identification was carried out by searching the Swiss-Prot protein database for Mus musculus using the MASCOT search engine of Matrix Science that integrated in the Global Protein Server Workstation. The mass tolerance was limited to 50 ppm. The results from both the MS and MS/MS spectra were accepted as a good identification when the GPS score confidence was higher than 95%.

2.6. Tissue samples and immunohistochemistry

Paraffin-embedded tumor tissues and normal adjacent tissues from Ruijin Hospital. The immunohistochemical analysis was performed on the 4 μm thick fraction mounted on charged slides and sectioned from each clinical sample. Then, each slide was deparaffinized in 60 °C, followed by treatment with xylene and graded alcohol. After the antigen retrieval and being blocked with 5% bovine serum albumin, tissue slides were immunohistochemically stained by antibodies against HIF-1α (Novus biologicals) and SOD2 (Epitomics), respectively, then visualized by standard avidin–biotinylated peroxidase complex method. Then, hematoxylin was used for counterstaining and morphologic images were observed with Olympus BX51 microscope.

All of staining was assessed by pathologists blinded to the origination of the samples and subject outcome. Each specimen was assigned a score according to the intensity of the staining as described [14] (no staining = 0; weak staining = 1, moderate staining = 2, strong staining = 3) and the extent of stained cells (0% = 0, 1–24% = 1, 25–49% = 2, 50–74% = 3, 75–100% = 4). The final immunoreactive score was determined by multiplying the intensity score with the extent of score of stained cells, ranging from 0 (the minimum score) to 12 (the maximum score).

2.7. qRT–PCR

Total RNA was isolated by TRIzol reagent (Invitrogen, Carlsbad, CA) and treated with RNase-free DNase (Promega, Madison, WI). Reverse transcription was performed with TaKaRa RNA PCR kit (TaKaRa, Dalian, China). The double-stranded DNA dye SYBR Green PCR Master Mixture Reagents (Applied Biosystems, Warrington, UK) was used for quantitative real-time reverse transcription–polymerase chain reaction (PCR) analysis as described previously [7]. The following specific primers used were 5'-GGACAAACCT-CAGCCCTAA-3' (forward) and 5'-TGAAACCAAGCCAACCC-3' (reverse) for SOD2, and 5'-CATCCTCACCCTGAAGTACCC-3' (forward) and 5'-AGCCTGGATAGCAACGTACATG-3' (reverse) for Actin as control. The folds of changes were shown as means ± SDs in three independent experiments with each triplicate.

2.8. shRNA design and transfection

Pairs of complementary oligonucleotides against VHL were synthesized, annealed and ligated into pSIREN-RetroQ according to the manufacturer's instruction (Clontech, Mountain View, CA). The target sequence for VHL was 5'-GAGCCTAGTCAAGCCTGAG-3' and the sequence for HIF-1α has been described previously [15]. Retroviruses were produced as previously described .After transfection for 48 h, the viral supernatant was collected, filter-sterilized and added to cells in six-well plate containing polybrane with a final concentration of 4 μg/ml and puromycin (2 μg/ml) was added to select the stably transfected cells after another 48 h.

2.9. Luciferase assay

The indicated sequences in promoter of SOD2 were obtained from National Center for Biotechnology Information, amplified by PCR from genomic DNA and subcloned into pGL3-Basic (Promega) to construct luciferase reporter plasmids. For the luciferase assay, 293T cells were seeded in a 12-well plate (Becton Dickinson, Franklin lakes, NJ), and cotransfected with pEF-BOS-HIF-1α, luciferase reporter plasmids driven by promoter fragments of SOD2 and pRLSV40-Renilla. After 24 h transfection, then put in normoxic or hypoxic conditions for another 12 h. Cells were lysed and analyzed by the Dual-Luciferase Assay system according to the manufacturer's instructions (Promega).

2.10. Chromatin immunoprecipitation

After grown under normoxia and hypoxia for 12 h, RCC4/VHL cells were crosslinked with 1% formaldehyde at room temperature for 10 min, and cells were pelleted and resuspended in 400 μl lysis buffer (1% sodium dodecyl sulphate, 10 mM ethylenediaminetetraacetic acid, 50 mM Tris–HCl, pH 8.0). Then DNA of the cells was sonicated and sheared to small fragments of 500–1000 bp with Sonicator ultrasonic processor (Misonix, Farmingdale, NY). Subsequently, the supernatant of the sonicated cells was collected, diluted and precleared by protein A agarose (Santa Cruz Biotechnology). Furthermore, anti-human HIF-1a monoclonal antibody (BD Transduction Laboratories, Lexington, KY) was added to the supernatant for immunoprecipitation with normal preimmuned mouse IgG (Santa Cruz Biotechnology) as a normal control. After overnight incubation, the protein A agarose were added and incubated for 3 h and then washed with low-salt, high-salt and LiCl buffers and the immunoprecipitated DNA was retrieved by 5M NaCl at 65 °C for 4 h and purified with a PCR purification kit

(TaKaRa). PCR for the HREs in the promotor was performed with specific primers: 5'-CCATCCTGACCAACATAGTG-3' (forward, P1) and 5'-TTGAGACACAGCCTCGCTCT-3' (reverse, P2) and 5'-TCATAGCTCATT GCAGCC-3' (forward, P3) and 5'-AGGTG-CAGTGGTTCATGCTT-3' (reverse, P4).

2.11. Western blot

Cell extracts were prepared by using the following lysis buffer (4% sodium dodecyl sulphate, 20% glycerol, 100 mM dithiothreitol, Tris–HCl, pH 6.8). Twenty micrograms of cell lysates were loaded and separated by 10 or 15% sodium dodecyl sulphate–polyacrylamide gel. After electrophoresis, proteins were transferred to nitrocellulose membrane (Bio-Rad, Richmond, CA). Then, 5% nonfat milk in Tris-buffered saline was used to block the membrane and immunoblotted with antibodies against Cox IV (Cell Signaling, Beverly, MA), Lamin B (Santa Cruz Biotech, Santa Cruz, CA), Actin (Merck, Darmstadt, Germany), HIF-1α (BD Transduction Laboratories), pVHL (Novus biologicals, Littleton, CO), PDK1 (stressgen) and SOD2 (Epitomics) .Followed by horseradish peroxidase-linked second antibody (Cell signaling Technology, Beverly, MA) for 1 h at room temperature, detection was performed by SuperSignal West Pico Chemiluminescent Substrate kit (Pierce, Rockford, IL) according to the manufacturer's instructions.

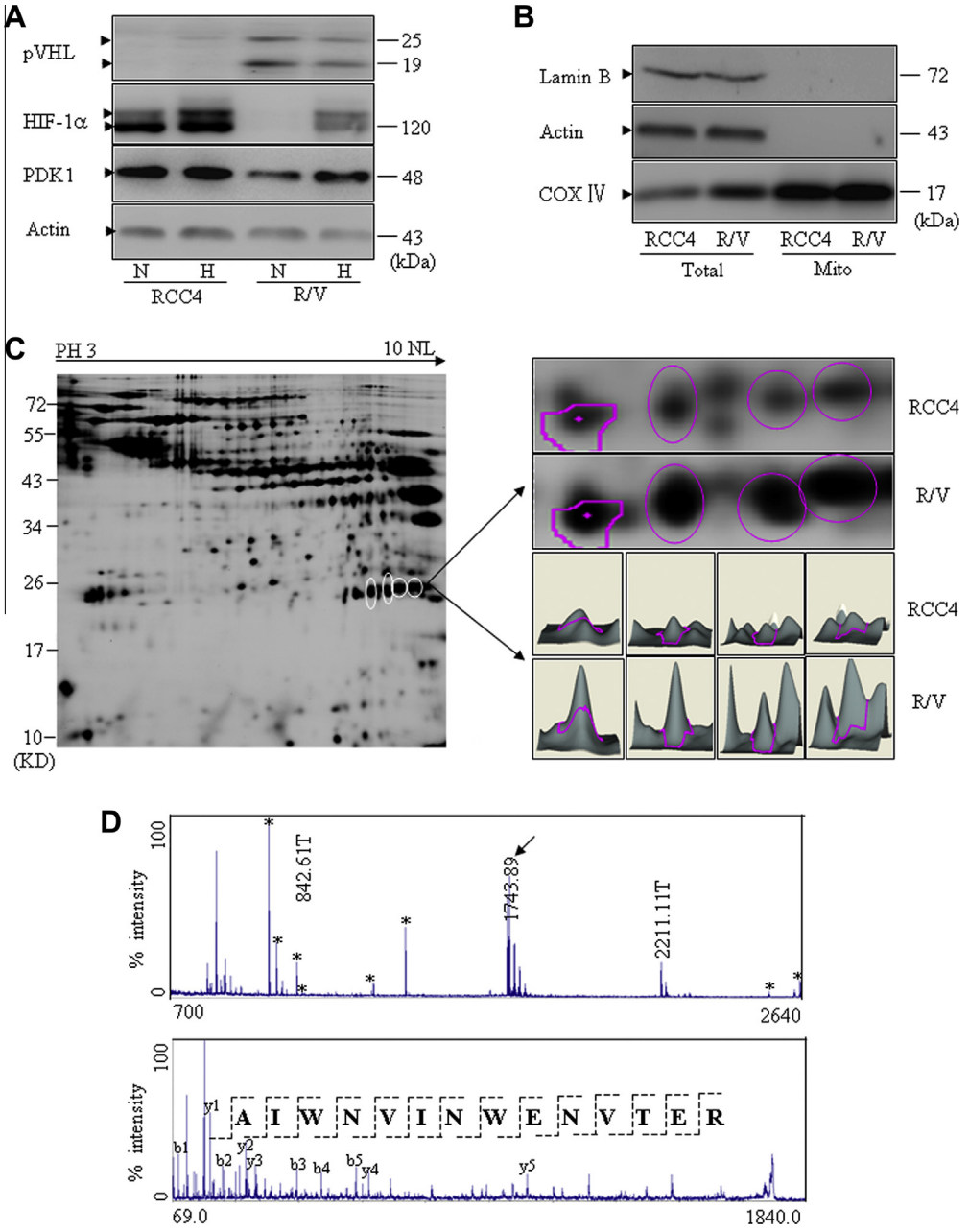

Fig. 1. SOD2 is identified by comparison of mitochondrial proteomes of RCC4 and RCC4/VHL. (A) RCC4 and RCC4/VHL were incubated in normoxia and hypoxia for 24 h. Indicated proteins were detected by Western blot. N and H represent normoxia and hypoxia. R/V represents RCC4/VHL. (B) Enrichment of mitochondria was verified by Western blot. "Total" and "Mito" represent whole cell extract and mitochondrial extract respectively. (C, left) Image of a representative 2-D DIGE gel. (C, right) Four spots were identified as SOD2 (top) and 3-D images of each spot visualized by the BVA module of DeCyder software were shown (bottom). (D) Peptide Mass Finger-printing spectrum of identified SOD2. "T" indicates trypsin autolytic peptides for internal calibration and asterisks indicate peaks matching SOD2 protein (top); A representative fragmentation spectrum (m/z = 1743.89) of MALDI-TOF-TOF tandem MS is shown with the insertion of the identified sequence. The identified sequence is AIWNVINWENVTER interpreted as y series and b series ions (bottom).

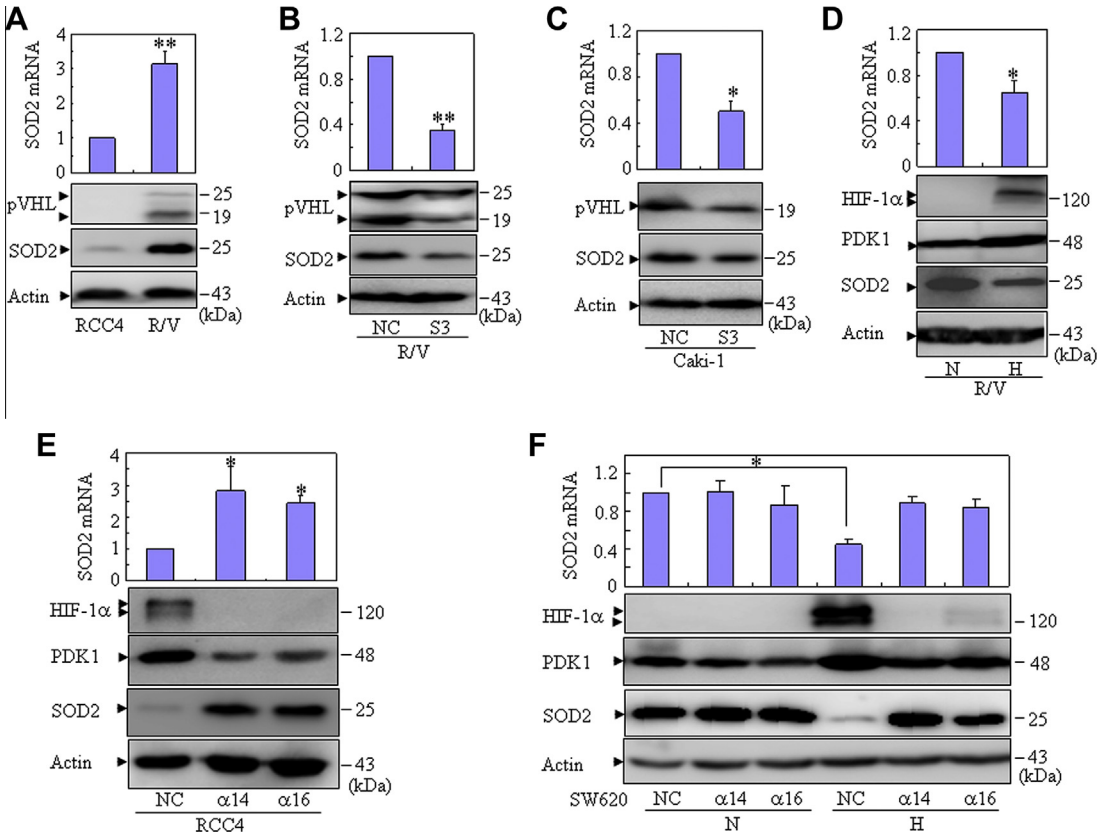

Fig. 2. SOD2 is regulated by HIF-1α. (A) The mRNA and protein levels of the indicated genes were respectively detected by real-time quantitative RT–PCR and Western blot in RCC4 and RCC4/VHL. (B and C) RCC4/VHL and Caki-1 cells were infected with retroviral vectors harboring shRNA against VHL (S3) or non-specific control (NC). The mRNA and protein levels of the indicated genes were respectively detected by real-time quantitative RT–PCR and Western blot. (D) RCC4/VHL cells were exposed to normal air or hypoxia (1% O2) for 12 h. The mRNA and protein levels of the indicated genes were respectively detected by real-time quantitative RT–PCR and Western blot. (E) RCC4 cells were stably transfected with shRNAs against HIF-1α (α14 and α16). The mRNA and protein levels of the indicated genes were respectively detected by real-time quantitative RT–PCR and Western blot. (F) SW620 cells transfected with shRNAs against HIF-1α (α14 and α16) were incubated in normoxia or hypoxia l for 12 h. The mRNA and protein levels of the indicated genes were respectively detected by real-time quantitative RT–PCR and Western blot. N and H represent normoxia and hypoxia. R/V represents RCC4/VHL. The column represents mean with bar as SD of three independent experiments with triplicate samples ($^{*}P < 0.05$; $^{**}P < 0.01$).

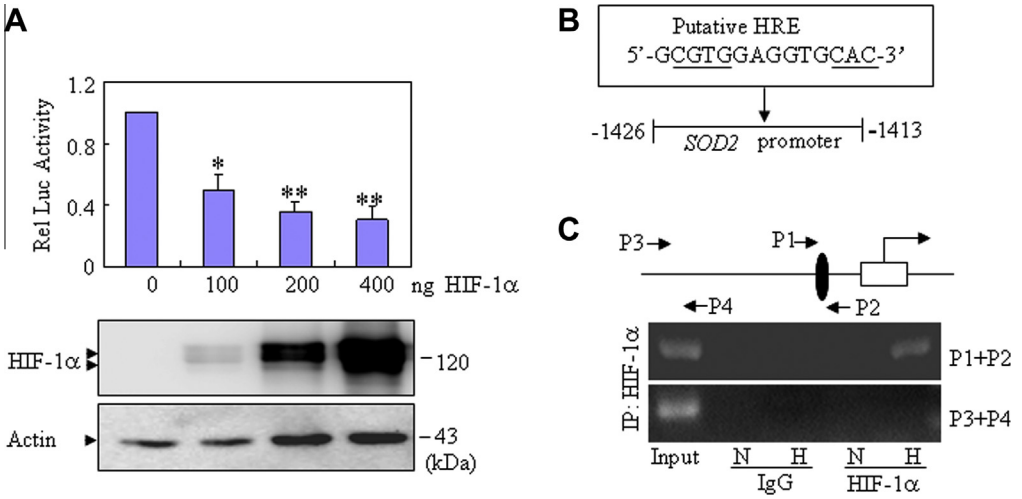

Fig. 3. The HRE in SOD2 promoter is essential for HIF-1α transactivity. (A) 293T cells were transfected with luciferase reporter plasmids containing the 2 kb SOD2 promoter together with the indicated doses of HIF-1α and cultured in normoxia for 36 h. The relative luciferase activities of SOD2 promoter were normalized by pSV40-Renilla and estimated as the relative folds against cells under normal air or empty vector-transfected cells. Protein levels of HIF-1α were detected by Western blot (low panel). All values represented the means with bar as SD of three independent experiments. (B) Scheme of the putative HRE in SOD2 promoter. (C) RCC4/VHL cells were grown under normoxia and hypoxia for 12 h. Chromatin immunoprecipitation assay was performed as described in Materials and methods. Black oval represents putative HRE.

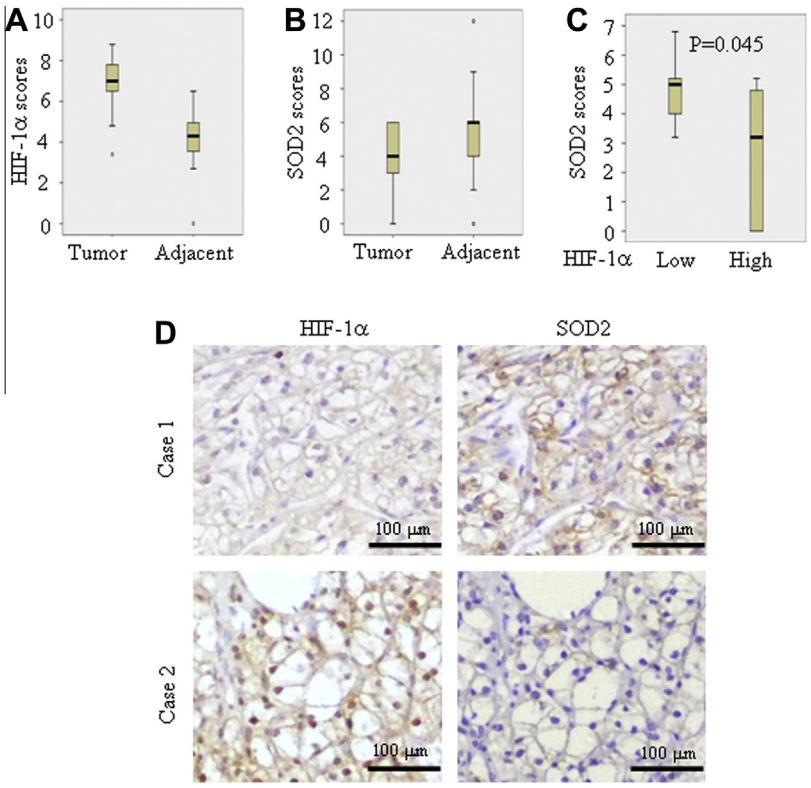

Fig. 4. Immunohistochemical analysis of renal clear cell carcinoma tumor tissues and normal adjacent tissues (A and B). HIF-1α (A) and SOD2 (B) expression scores are shown as box plots, with the horizontal lines representing the median; the bottom and top of the boxes representing the 25th and 75th percentiles, respectively; and the vertical bars representing the range of data. We compared renal clear cell carcinoma tissues with matched adjacent normal tissues ($n = 20$). Any outliers are marked with a circle. (C) Box plot of SOD2 expression in renal clear cell carcinoma from 20 subjects. The subjects were divided into two groups based on HIF-1α expression scores in the tumors, representing low (scores 0–6), high (scores 6–12) expression of HIF-1α. Data was analyzed by one-way ANOVA test with Games-Howell's correction [14]. (D) Morphologic illustrations of representative immunohistochemical stainings of HIF-1α and SOD2 in the same tumor tissues.

2.12. Statistical analysis

All experiments were repeated at least for three times with the same results. The Student's *t*-test was used to compare the difference between two different groups. $P < 0.05$ was considered to be statistically significant. The results of immunohistochemistry were analyzed by SAS Enterprise software (SAS Institute, Cary, NC) as indicated.

3. Results

3.1. The expression of SOD2 is significantly reduced in pVHL deficient renal clear cell carcinoma cell line RCC4

RCC4, a pVHL defective cell line derived from sporadic renal clear cell carcinoma (CCRCC), expresses HIF-1α in nomoxia. In order to find mitochondrial targets of HIF-1α, RCC4 and RCC4 with stable re-expression of pVHL (RCC4/VHL) were used [4]. As shown in Fig. 1A, by Western blot, we confirmed that RCC4/VHL cells expressing wild-type pVHL accumulated lower levels of HIF-1α and the HIF-1α responsive gene PDK1 than RCC4 cells in normoxia. However, when RCC4/VHL cells were cultured in hypoxia, HIF-1α and PDK1 were up-regulated. Mitochondria were isolated from both cells and verified with the enrichment of mitochondrial protein Cox IV. No significant contamination of nuclear or cytosolic proteins was observed as evidenced by detection of nuclear protein Lamin B and cytosolic protein Actin (Fig. 1B). Then, mitochondrial protein extracts were applied to comparative analysis by 2D-DIGE. Fig. 1C (left) shows a representative gel. All the differential spots were cut from preparative gel, digested and applied to MALDI-TOF-TOF tandem MS analysis. Four spots were found to be dramatically up-regulated in RCC4/VHL (Fig. 1C, right), all of which were identified as SOD2 by MALDI-TOF/TOF PMF and MS/MS analysis (Fig. 1D).

3.2. VHL regulates SOD2 through HIF-1

Next we sought to confirm the result of 2D-DIGE. As shown in Fig. 2A, our results demonstrated that SOD2 mRNA and protein levels were significantly up-regulated in RCC4/VHL compared with RCC4. Then, in order to verify the regulation of pVHL upon SOD2, we stably transfected shRNA specifically against pVHL (S3) together with a scrambled shRNA (NC) into RCC4/VHL and another renal clear cell carcinoma cell line Caki-1 in which VHL is normally expressed. Accordingly, silencing of pVHL suppressed SOD2 expression on mRNA and protein levels (Fig. 2B and C). HIF-1α is one of the most important transcription factors regulated by VHL. We supposed that HIF-1α might be involved in this process. Thus, we cultured RCC4/VHL cells in normoxia and hypoxia respectively for 12 h. The results showed that hypoxia decreased the mRNA and protein levels of SOD2 (Fig. 2D). Next, we stably transfected shRNAs specifically against HIF-1α (α14 and α16), together with NC into RCC4 cells. As shown in Fig. 2E, both α14 and α16 but not NC shRNA significantly suppressed HIF-1α and PDK1. Notably, α14 and α16 also increased SOD2 mRNA and protein (Fig. 2E). Furthermore, we knocked down HIF-1α in colon cancer cell line SW620 cells [8], and cultured these cells in normoxia and hypoxia for 12 h. The results showed that hypoxia inhibited SOD2 expression at both mRNA and protein levels, while knockdown of HIF-1α restored it (Fig. 2F). Totally, these results suggested that

HIF-1α mediated the transcriptional suppression of SOD2 in the pVHL deficient cells.

3.3. HIF-1 directly binds the HRE of SOD2 promoter

In order to find out whether HIF-1α regulates SOD2 expression through direct mechanisms, we subcloned a 2 kb DNA fragment upstream of the transcriptional start site of SOD2 into a luciferase report vector pGL3-basic, which was subsequently co-transfected into 293T cells with a gradient of HIF-1α plasmid and the internal control Renilla. Thirty-six hours later, we found that the luciferase activity of SOD2 promoter was inhibited in a dose-dependent manner by the ectopic expression of HIF-1α protein (Fig.3A). Bioinformatic analysis indicated one potential HRE within the 2 kb region (Fig. 3B), which was consolidated by chromatin immunoprecipitation assay in hypoxia-incubated RCC4/VHL cells. As shown in Fig. 3C, anti-HIF-1α antibody but not normal mouse IgG could precipitate the putative HRE.

3.4. The expression of HIF-1 negatively correlates with SOD2 in pVHL deficient renal clear cell carcinoma tissues

To further demonstrate the regulational relationship between HIF-1α and SOD2, we did immunohistochemical analysis with the tumor tissues and normal adjacent tissues from 20 cases of renal clear cell carcinoma patients. As shown in Fig. 4A and B, significantly higher expression of HIF-1α were found in cancer tissues compared to their corresponding adjacent tissues. Notably, down-regulation of SOD2 was found in the same cancer tissues. In addition, the correlation of HIF-1α and SOD2 in the cancer tissues was further investigated. As shown in Fig. 4C and D, high HIF-1α expression is often associated with low SOD2 expression, and vice versa ($P < 0.05$). Taken together, these results suggest that SOD2 expression has a negative correlation with HIF-1α expression.

4. Discussion

The expression of HIF-1α in CCRCC is higher than normal tissues because VHL is mutated or silenced in >50% of renal clear cell carcinoma. From our results, we find that renal clear cell carcinoma cell lines and tissues present lower expression of SOD2. HIF-1α is therefore proposed and verified to be the mediator for the suppression of SOD2. It is well known that hypoxic condition increases intracellular ROS level. ROS, a byproduct of mitochondrial respiration, acts not only as a damaging oxidant but also a signaling molecule. ROS signaling is involved in some crucial biologic processes such as cell proliferation and differentiation [9]. HIF-1α is known to suppress mitochondria function as well as ROS production. The down-regulation of SOD2 may be an important mechanism to balance ROS production and dismutation to maintain a proper level of ROS for the prosperous proliferation of cancer cells.

Low expression of SOD2 has been found in other tumors [16,17] . In these solid tumors whose pVHL is normally expressed, the positive feedback between HIF-1α and SOD2 might result in a constant and quick response to hypoxia of cancer cells. The possible molecular mechanism might be as follows. Hypoxia induces the expression of HIF-1α, which then leads to the down-regulation of SOD2 and thus the accumulation of ROS. The increased ROS promotes HIF-1α stabilization.

As a transcription factor, the main role of HIF-1α is transcriptional activation of its target genes. But it can also function as a transcriptional repressor. It can repress some target genes such as PPARα and Bax through transcription inactivation [18,19]. Our result that HIF-1α inhibits SOD2 expression provides new clue on the role of HIF-1α as a transcriptional repressor.

Acknowledgments

This work is supported in part by grants from National Natural Science Foundation of China (NSFC, Nos. 31170783, 81071668), Science and Technology Commission of Shanghai (11QH1401700).

References

[1] W.G. Kaelin Jr., P.J. Ratcliffe, Oxygen sensing by metazoans: the central role of the HIF hydroxylase pathway, Mol. Cell 30 (2008) 393–402.
[2] G.L. Wang, B.H. Jiang, E.A. Rue, G.L. Semenza, Hypoxia-inducible factor 1 is a basic-helix-loop-helix-PAS heterodimer regulated by cellular O_2 tension, Proc. Natl. Acad. Sci. USA 92 (1995) 5510–5514.
[3] R. Fukuda, B. Kelly, G.L. Semenza, Vascular endothelial growth factor gene expression in colon cancer cells exposed to prostaglandin E2 is mediated by hypoxia-inducible factor 1, Cancer Res. 63 (2003) 2330–2334.
[4] I. Papandreou, R.A. Cairns, L. Fontana, A.L. Lim, N.C. Denko, HIF-1 mediates adaptation to hypoxia by actively downregulating mitochondrial oxygen consumption, Cell Metab. 3 (2006) 187–197.
[5] J.W. Kim, I. Tchernyshyov, G.L. Semenza, C.V. Dang, HIF-1-mediated expression of pyruvate dehydrogenase kinase: a metabolic switch required for cellular adaptation to hypoxia, Cell Metab. 3 (2006) 177–185.
[6] C.M. Tang, J. Yu, Hypoxia-inducible factor-1 as a therapeutic target in cancer, J. Gastroenterol. Hepatol. 28 (2013) 401–405.
[7] S.H. Liao, X.Y. Zhao, Y.H. Han, J. Zhang, L.S. Wang, L. Xia, K.W. Zhao, Y. Zheng, M. Guo, G.Q. Chen, Proteomics-based identification of two novel direct targets of hypoxia-inducible factor-1 and their potential roles in migration/invasion of cancer cells, Proteomics 9 (2009) 3901–3912.
[8] X.Y. Zhao, T.T. Chen, L. Xia, M. Guo, Y. Xu, F. Yue, Y. Jiang, G.Q. Chen, K.W. Zhao, Hypoxia inducible factor-1 mediates expression of galectin-1: the potential role in migration/invasion of colorectal cancer cells, Carcinogenesis 31 (2010) 1367–1375.
[9] M. Rigoulet, E.D. Yoboue, A. Devin, Mitochondrial ROS generation and its regulation: mechanisms involved in H(2)O(2) signaling, Antioxid. Redox Signal. 14 (2010) 459–468.
[10] R.D. Guzy, P.T. Schumacker, Oxygen sensing by mitochondria at complex III: the paradox of increased reactive oxygen species during hypoxia, Exp. Physiol. 91 (2006) 807–819.
[11] E.L. Bell, T.A. Klimova, J. Eisenbart, C.T. Moraes, M.P. Murphy, G.R. Budinger, N.S. Chandel, The Qo site of the mitochondrial complex III is required for the transduction of hypoxic signaling via reactive oxygen species production, J. Cell Biol. 177 (2007) 1029–1036.
[12] E. Sasabe, Z. Yang, S. Ohno, T. Yamamoto, Reactive oxygen species produced by the knockdown of manganese-superoxide dismutase up-regulate hypoxia-inducible factor-1alpha expression in oral squamous cell carcinoma cells, Free Radic. Biol. Med. 48 (2010) 1321–1329.
[13] S.M. Shen, Y. Yu, Y.L. Wu, J.K. Cheng, L.S. Wang, G.Q. Chen, Downregulation of ANP32B, a novel substrate of caspase-3, enhances caspase-3 activation and apoptosis induction in myeloid leukemic cells, Carcinogenesis 31 (2010) 419–426.
[14] X. Pan, T. Zhou, Y.H. Tai, C. Wang, J. Zhao, Y. Cao, Y. Chen, P.J. Zhang, M. Yu, C. Zhen, R. Mu, Z.F. Bai, H.Y. Li, A.L. Li, B. Liang, Z. Jian, W.N. Zhang, J.H. Man, Y.F. Gao, W.L. Gong, L.X. Wei, X.M. Zhang, Elevated expression of CUEDC2 protein confers endocrine resistance in breast cancer, Nat. Med. 17 (2011) 708–714.
[15] L.P. Song, J. Zhang, S.F. Wu, Y. Huang, Q. Zhao, J.P. Cao, Y.L. Wu, L.S. Wang, G.Q. Chen, Hypoxia-inducible factor-1alpha-induced differentiation of myeloid leukemic cells is its transcriptional activity independent, Oncogene 27 (2008) 519–527.
[16] Y. Soini, M. Vakkala, K. Kahlos, P. Paakko, V. Kinnula, MnSOD expression is less frequent in tumour cells of invasive breast carcinomas than in in situ carcinomas or non-neoplastic breast epithelial cells, J. Pathol. 195 (2001) 156–162.
[17] L.Y. Yang, W.L. Chen, J.W. Lin, S.F. Lee, C.C. Lee, T.I. Hung, Y.H. Wei, C.M. Shih, Differential expression of antioxidant enzymes in various hepatocellular carcinoma cell lines, J. Cell Biochem. 96 (2005) 622–631.
[18] S. Narravula, S.P. Colgan, Hypoxia-inducible factor 1-mediated inhibition of peroxisome proliferator-activated receptor alpha expression during hypoxia, J. Immunol. 166 (2001) 7543–7548.
[19] J.T. Erler, C.J. Cawthorne, K.J. Williams, M. Koritzinsky, B.G. Wouters, C. Wilson, C. Miller, C. Demonacos, I.J. Stratford, C. Dive, Hypoxia-mediated down-regulation of Bid and Bax in tumors occurs via hypoxia-inducible factor 1-dependent and -independent mechanisms and contributes to drug resistance, Mol. Cell Biol. 24 (2004) 2875–2889.